Available online at www.sciencedirect.com
SCIENCE DIRECT
Journal of Catalysis 237 (2006) 255–266
JOURNAL OF CATALYSIS
www.elsevier.com/locate/jcat

Reaction kinetics and in situ sum frequency generation surface vibrational spectroscopy studies of cycloalkene hydrogenation/dehydrogenation on Pt(111): Substituent effects and CO poisoning

Minchul Yang [a], R.M. Rioux [a,b], G.A. Somorjai [a,b,*]

[a] *Department of Chemistry, University of California, Berkeley, CA 94720, USA*
[b] *Materials Science Division, Lawrence Berkeley National Laboratory, Berkeley, CA 94720, USA*

Received 30 August 2005; revised 21 October 2005; accepted 24 October 2005

Available online 13 December 2005

Abstract

The influence of substituent effects and CO poisoning were examined during the hydrogenation/dehydrogenation of cycloalkenes (cyclohexene and 1- and 4-methylcyclohexene) on a Pt(111) single crystal. Reaction rates for both hydrogenation and dehydrogenation decreased when a methyl group was added to the cycloalkene ring. The location of a methyl group relative to the C=C double bond was influential in the overall kinetics for both reaction pathways. All cycloalkenes demonstrated "bend-over" Arrhenius behavior, after which rates for hydrogenation and dehydrogenation decreased with increasing temperature (inverse Arrhenius behavior). This is explained in terms of a change in surface coverage of the reactive cycloalkene. The potential importance of hydrogen effects is discussed. Introduction of CO in the Torr pressure range (0.015 Torr) led to a decrease in turnover frequency and increase in apparent activation energy for both the hydrogenation and dehydrogenation of all cycloalkenes. Sum frequency generation (SFG) surface vibrational spectroscopy revealed that upon adsorption, the three cycloalkenes form a surface species with similar molecular structure. SFG results under reaction conditions in the presence of CO demonstrated that the cycloalkene coverage is low on a CO-saturated surface. Substituted cyclohexenes were more sensitive than cyclohexene to the presence of adsorbed CO, with larger increases in the apparent activation energy, especially in the case of dehydrogenation. A qualitative explanation for the changes in activity with temperature and the increase in apparent activation energy for cycloalkene hydrogenation/dehydrogenation in the presence of CO is presented from a thermodynamic and kinetic perspective.

Keywords: Cycloalkene; Hydrogenation; Dehydrogenation; Pt(111); Co poisoning; Substituent effects; Sum frequency generation

1. Introduction

Chemical reactions of cycloalkenes on metal surfaces have attracted considerable interest due to their importance in many aspects of heterogeneous hydrocarbon conversion chemistry including hydrogenation, dehydrogenation, ring opening, and isomerization. The hydrogenation and dehydrogenation reactions of cycloalkenes have been widely used as a model system for fundamental studies of catalysis and a testing ground for new heterogeneous catalysts [1–5]. For some cycloalkenes, their dehydrogenation reactions are considered a major step in the dehydrocyclization of *n*-alkanes to aromatics, an important reaction in the catalytic-reforming process [6]. Cyclohexene (C_6H_{10}) is one of most extensively studied cycloalkenes.

Cyclohexene adsorption on Pt(111) at low pressures ($<10^{-6}$ Torr) has been studied using various surface-analytical techniques, including thermal desorption spectroscopy (TDS) [7], bismuth postdosing TDS (BPTDS) [7,8], laser-induced thermal desorption (LITD) [9], high-resolution electron energy loss spectroscopy (HREELS) [9,10], and reflection absorption infrared spectroscopy (RAIRS) [11]. Cyclohexene exists in a di-σ form on Pt(111) at 100 K, converting to π-allyl c-C_6H_9 at ∼200 K [8,11]. At ∼300 K, π-allyl c-C_6H_9 converts to benzene. Further heating induces desorption and decomposition of benzene [8,9,11]. Cyclohexene surface reactions on Pt(111) at

* Corresponding author. Fax: +1 510 643 9668.
E-mail addresses: somorjai@berkeley.edu, somorjai@socrates.berkeley.edu (G.A. Somorjai).

0021-9517/$ – see front matter © 2005 Published by Elsevier Inc.
doi:10.1016/j.jcat.2005.10.025

high pressure (1.5 Torr) was also studied by sum frequency generation (SFG) vibrational spectroscopy [12]. Various surface species were observed during the reactions in the range of 303–483 K. On adsorption at 303 K, cyclohexene is dehydrogenated to form 1,4-cyclohexadiene (C_6H_8). At 323 K, this species converts to π-allyl c-C_6H_9 intermediate. At temperatures above 423 K, benzene coexists with C_6H_9 on the surface. Kinetic studies of cyclohexene hydrogenation/dehydrogenation reactions on Pt(111) have also been reported [13,14].

In this study, substituent effects by methyl groups and poisoning effects of coadsorbed CO on the hydrogenation/dehydrogenation reactions of cycloalkenes (cyclohexene and 1- and 4-methylcyclohexenes) on Pt(111) were investigated. Substituent effects, concerning the chemical effect of functional groups replacing hydrogen atoms on reactivity, can greatly influence activity and selectivity in catalytic reactions [15–17]. The poisoning of catalysts, either intentionally or unintentionally, can have a dramatic effect on catalytic activity and selectivity [18–21].

An example of intentional poisoning is the addition of sulfur to platinum hydrocarbon conversion catalysts. Sulfur is added to commercial naphtha-reforming catalysts (Pt/Al_2O_3) to suppress excessive hydrogenolysis. It is postulated that sulfur adsorbs irreversibly to coordinatively unsaturated surface atoms or restructures the surface [18]. A reaction in which products adsorbs very strongly to the catalyst surface and inhibits further turnover is an example of unintentional self-poisoning. Catalyst poisons are often introduced to catalysts from feedstocks containing a low level of the poison but a sufficient level to deactivate catalysts. Few studies have been conducted on the influence of CO poisoning on hydrocarbon conversion reactions [19–23]. Adding CO in the Torr range during ethylene hydrogenation led to a doubling of the apparent activation energy on Pt(111) [21–23], whereas similar CO pressures had little influence on the apparent activation energy on Pt nanoparticle arrays [23], but both catalysts exhibited a several order of magnitude decrease in activity. Damiani and Butt [19,20] used the hydrogenolysis of methylcyclopropane as a probe reaction to investigate the structure sensitivity of the deactivation of Pt/Al_2O_3 and Pt/TiO_2 catalysts by CO. They demonstrated that larger Pt particles supported on Al_2O_3 were more sensitive to CO poisoning than smaller particles, whereas TiO_2-supported catalysts were more susceptible to CO poisoning than the Al_2O_3 supported catalysts regardless of Pt particle size.

Kinetic studies were conducted to measure reaction rates and apparent activation energies for the three cycloalkenes in the absence and presence of CO. Comparative studies between the three cycloalkenes demonstrated that the hydrogenation/dehydrogenation reaction rates were strongly affected by the existence of alkyl group and its proximity to the C=C double bond. Adding an alkyl group to the cycloalkene ring had a significant effect on overall catalytic activity but little effect on the selectivity to either product. Both reactions were poisoned by coadsorbed CO for all three cycloalkenes and led to an increase in the apparent activation energy. The change in the apparent activation energy due to CO poisoning were similar for the hydrogenation and the dehydrogenation of cyclohexene and 1-methylcyclohexene, but significantly greater for the dehydrogenation of 4-methylcyclohexene. In addition, SFG vibrational studies were carried out to identify surface intermediates during the hydrocarbon conversion reactions. Based on kinetic and SFG results, we discuss substituent and CO poisoning effects on cycloalkene hydrogenation/dehydrogenation reactions. A qualitative explanation for the changes in activity with temperature and the increase in apparent activation for cycloalkene hydrogenation/dehydrogenation in the presence of CO is discussed from a mechanistic standpoint.

2. Experimental

All experiments were carried out on a Pt(111) single-crystal surface in a high-pressure/ultrahigh-vacuum (HP/UHV) system. The HP/UHV system comprises a UHV chamber with a base pressure of 4×10^{-10} Torr and a high-pressure cell in which high-pressure catalysis studies were carried out. The HP cell was equipped with a reaction loop containing a recirculation pump and a septum for gas abstraction and gas chromatography (GC) analysis. For GC measurements, a recirculation pump constantly mixed the reactant and product gases in the HP cell, and periodic sampling allowed measurements of the gas-phase composition. All kinetic studies were carried out in 1.5 Torr cycloalkenes (cyclohexene and 1- and 4-methylcyclohexenes) and 15 Torr H_2 in the presence or absence of 0.015 Torr CO in the temperature range 295–530 K. Reactions were typically run for 30 min; initial turnover rates (TORs) were calculated from accumulation plots (C_6H_{12} or C_6H_6 turnover number vs time).

For SFG experiments, a mode-locked 20-ps, 20-Hz Nd:YAG laser with a 25-mJ/pulse energy output at 1064 nm was used to generate a tunable infrared beam at 1300–3200 cm^{-1} and a visible beam at 532 nm. The visible (200 μJ/pulse) and the infrared (100 μJ/pulse) beams were spatially and temporally overlapped on the Pt(111) surface with incident angles of 55° and 60°, respectively, with respect to surface normal. Both the infrared and visible beams were p-polarized. As the infrared beam is scanned over the frequency range of interest, the p-polarized sum frequency output from the Pt(111) crystal was collected by a photomultiplier and a gated integrator.

The theory of SFG for surface studies has been described in detail previously [24–26]. Briefly, SFG is a second-order nonlinear optical process in which an infrared laser beam at ω_{IR} is combined with a visible laser beam at ω_{VIS} to generate a sum frequency output at $\omega_{SF} = \omega_{IR} + \omega_{VIS}$. This process is allowed only in a medium without centrosymmetry under the electric dipole approximation. Platinum bulk is centrosymmetric, and its contribution to SFG is usually negligible. Isotropic gases in the HP cell do not generate SFG; only the metal surface and adsorbates on the surface can generate SFG under the electric dipole approximation. The SFG signal, I_{SF}, is related to the incident visible (I_{VIS}) and infrared (I_{IR}) beam intensities, and to the second-order susceptibility of the media ($\chi^{(2)}$), as

$$I_{SF} \propto |\chi^{(2)}|^2 I_{VIS} I_{IR}. \quad (1)$$

Near resonance with vibrational modes of the adsorbates, the second-order susceptibility $\chi^{(2)}$ is given by

$$\chi^{(2)} = \chi_{\mathrm{NR}} + \sum_q \frac{A_q}{\omega_{\mathrm{IR}} - \omega_q + i\Gamma_q}, \quad (2)$$

where χ_{NR} is the nonresonance contribution and A_q, ω_q, and Γ_q denote the vibrational mode strength, resonant frequency, and line width of the qth vibrational mode, respectively. The nonresonance contribution, χ_{NR}, originates from the metal surface and is usually independent of the frequency of the infrared laser beam. In contrast, the second term is significantly enhanced when the frequency of the infrared laser beam is in resonance with a vibrational mode of the adsorbates. The vibrational mode strength, A_q, is proportional to the surface density of the adsorbates, and infrared and Raman transition cross-sections of the qth vibrational mode.

To analyze the SFG spectrum, the SFG signal, I_{SF}, was first normalized to the intensity (I_{IR}) of the incident infrared beam on the surface. This is necessary because gas molecules in the HP cell absorb some portion of the incident infrared beam, to which I_{SF} is linearly proportional, as described in Eq. (1). Detailed descriptions of the HP/UHV system and SFG measurement have been provided previously [27,28].

The Pt(111) crystal was cleaned by sputtering with Ar^+ ions (1 keV), heating at 900 K in the presence of 5×10^{-7} Torr O_2 for 2 min, then annealing at 1200 K in UHV for 2 min. After a few cycles of cleaning, the Pt(111) crystal was transferred to the HP cell for SFG or GC measurements. The Pt(111) surface was routinely checked by Auger electron spectroscopy (AES) for cleanliness. Cyclohexene, 1-methylcyclohexene, and 4-methylcyclohexene (⩾99.5%, Aldrich) were purified by several freeze–pump–thaw cycles before being introduced into the HP cell.

3. Results and analysis

3.1. Kinetic study of cycloalkene (cyclohexene and 1- and 4-methylcyclohexenes) hydrogenation/dehydrogenation reactions on Pt(111)

Hydrogenation and dehydrogenation of cyclohexene led to the production of cyclohexane and benzene, respectively, whereas hydrogenation and dehydrogenation of 1- and 4-methylcyclohexene led to the production of methylcyclohexane and toluene, respectively. Fig. 1 shows the temperature dependence of the initial TOR, in molecules per Pt atom per second, for the hydrogenation and dehydrogenation of cyclohexene, 1-methylcyclohexene, and 4-methylcyclohexene.

In the absence of CO, the temperature dependence of the TORs is similar for the three cycloalkenes. Cycloalkene hydrogenation rates increase with temperature before reaching a maximum at ∼390 K and finally decreasing as the temperature is increased. In the case of cycloalkene dehydrogenation, the onset of dehydrogenation begins at ∼350 K and increases until maximum activity is achieved at ∼450 K. The decreased catalytic activity at higher temperatures for both hydrogenation and dehydrogenation is explained in terms of a change in the surface coverage of adsorbed cycloalkene species due to unfavorable adsorption thermodynamics. Maximum catalytic activity increases in the order 1-methylcyclohexene < 4-methylcyclohexene < cyclohexene. For example, at standard conditions of 1.5 Torr cycloalkene, 15 Torr H_2, and 390 K, the cycloalkene hydrogenation rate is 7.0 molecules site^{-1} s^{-1} for cyclohexene and 3.6 and 0.73 molecules site^{-1} s^{-1} for 1- and 4-methylcyclohexene, respectively. This trend is explained by steric hindrance of the methyl group on the cycloalkene and its proximity to the double bond.

TORs for hydrogenation and dehydrogenation of the three cycloalkenes were significantly reduced in the presence of CO (Fig. 1). For hydrogenation, the temperatures corresponding to maximum activities shifted from ∼400 to ∼460 K, and maximum activities (or TORs) were reduced by 60–85% in the presence of CO. For dehydrogenation, the temperatures corresponding to maximum activity shifted from ∼450 to ∼510 K, and maximum activities were reduced by 18–30% in the presence of CO. At low temperatures, the rate of both hydrogenation and dehydrogenation behave in an Arrhenius fashion. Arrhenius plots for both cycloalkene hydrogenation and dehydrogenation in the presence and absence of CO are shown in Fig. 2. The apparent activation energies for both reactions are compiled in Table 1. The quantity ΔE_{app} is defined as the difference in apparent activation energy in the presence and absence of CO, or $\Delta E_{\mathrm{app}} = E_{\mathrm{app}}$ (with CO) $- E_{\mathrm{app}}$ (without CO). In the absence of CO, E_{app}'s for the hydrogenation are 3.7–8.6 kcal mol^{-1}, whereas E_{app} for dehydrogenation are 15.2–19.7 kcal mol^{-1}. The presence of CO increases E_{app} by 6.0–14.8 kcal mol^{-1}. For cyclohexene, ΔE_{app} (7.5 kcal mol^{-1}) for hydrogenation is almost identical to ΔE_{app} (6.9 kcal mol^{-1}) for dehydrogenation within experimental uncertainties. The similarity between ΔE_{app}'s for hydrogenation and dehydrogenation holds in the case of 1-methylcyclohexene (9.4 and 8.1 kcal mol^{-1}, respectively). In contrast, 4-methylcyclohexene shows a noticeable difference in ΔE_{app} for the hydrogenation and the dehydrogenation (6.0 and 14.8 kcal mol^{-1}, respectively). The reason for the large increase in the apparent activation energy for 4-methylcyclohexene dehydrogenation is not clear, but may be related to the lack of large ensembles of surface atoms required for double-bond migration upon adsorption because of the high CO coverage.

3.2. SFG vibrational spectra of surface species on adsorption of cycloalkenes on Pt(111) at 403 K

SFG vibrational spectra of cyclohexene derived surface species on Pt(111) at 403 K under 1.5 Torr cycloalkenes and 15 Torr H_2 are shown in Fig. 3. The SFG spectrum of cyclohexene, which has been previously reported from our laboratory [12], is presented here for comparison with those of 1- and 4-methylcyclohexene. In the case of cyclohexene, two major bands, at 2840 and 2920 cm^{-1}, are assigned to symmetric and antisymmetric C–H stretches of a CH_2 group, respectively, and the corresponding surface species is π-allyl c-C_6H_9 [12]. A proposed molecular structure of π-allyl c-C_6H_9 is illustrated in Scheme 1a. The CH_2 groups at C_3, C_4, and C_5 positions can

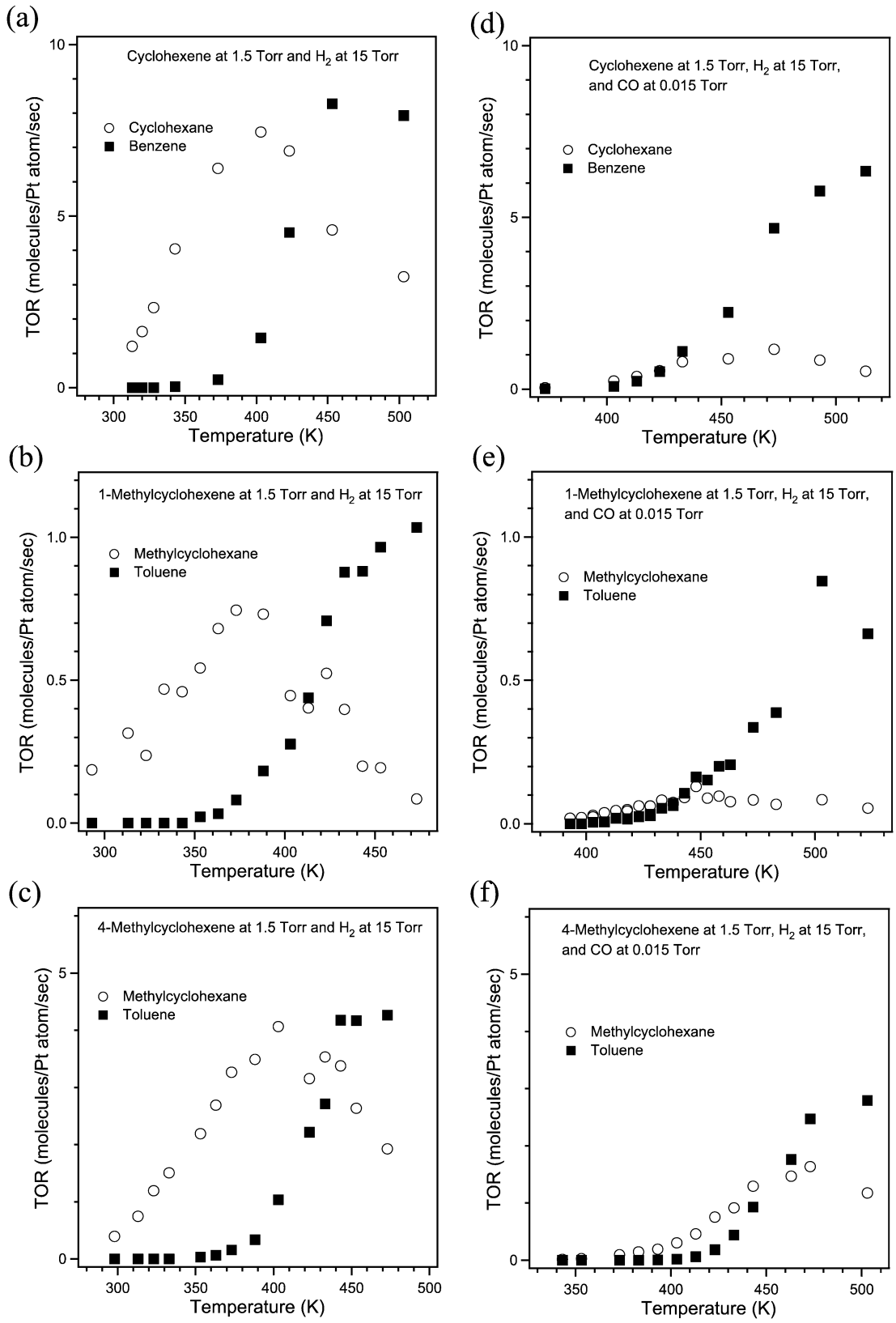

Fig. 1. Temperature dependence of initial turnover rates (TORs), in molecules per Pt atom per second, for hydrogenation and dehydrogenation of cyclohexene, 1-methylcyclohexene, and 4-methylcyclohexene. Empty circles and filled squares represent the TORs for hydrogenation and dehydrogenation, respectively. All kinetics studies were carried out at 1.5 Torr cycloalkenes and 15 Torr H_2 in the absence (a–c) or presence (d–f) of 0.015 Torr CO.

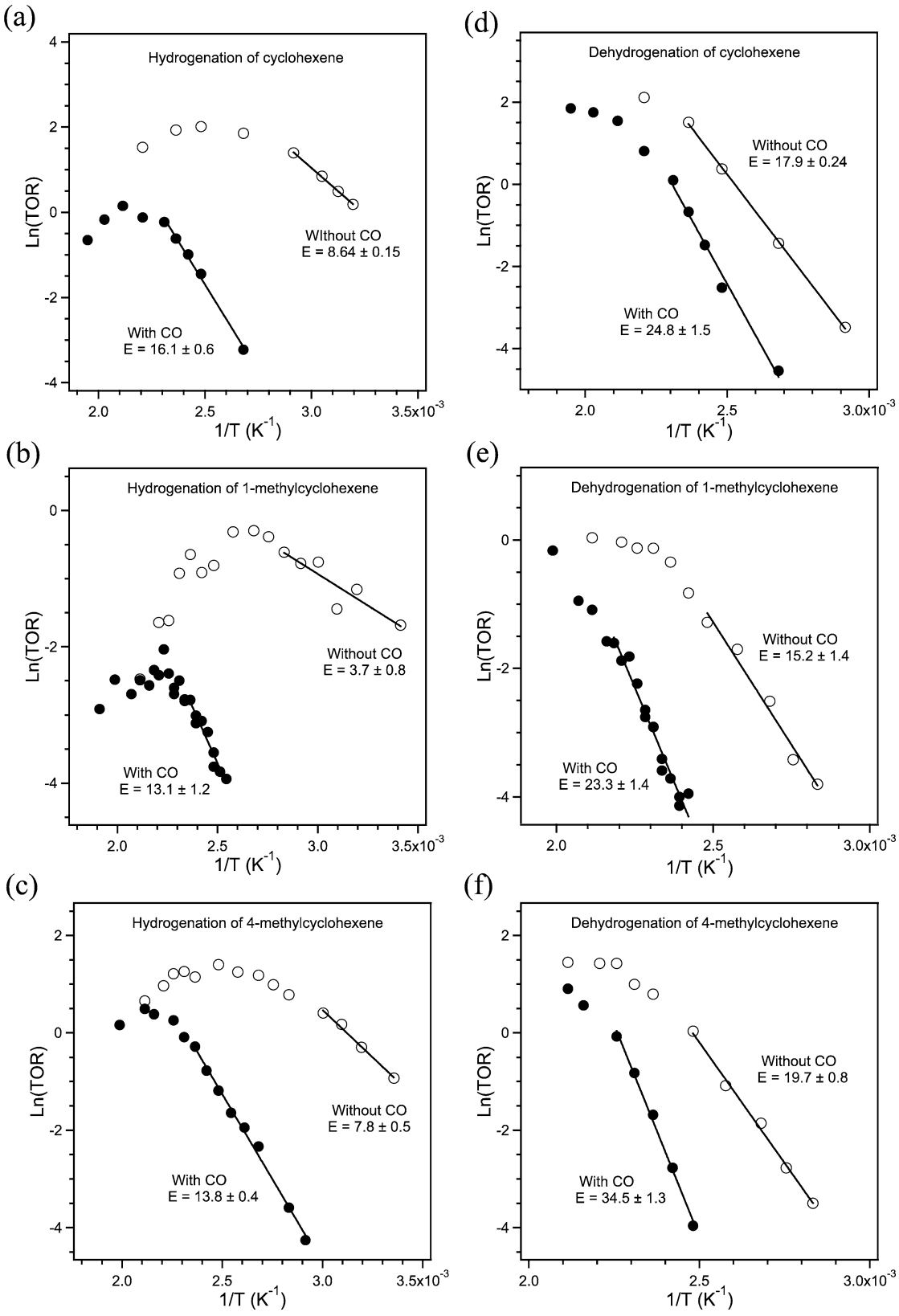

Fig. 2. Arrhenius plots for cycloalkene hydrogenation (a–c) and dehydrogenation (d–f). Empty and filled circles represent the TORs in the absence and presence of CO, respectively, and solid lines represent the linear fit of the logarithm of TOR with respect to $1/T$.

Table 1
Apparent activation energy (E_{app}, in kcal mol^{-1}) for cycloalkene hydrogenation/dehydrogenation

	Cyclohexene		1-Methylcyclohexene		4-Methylcyclohexene	
	Without CO	With CO	Without CO	With CO	Without CO	With CO
Hydrogenation						
E_{app}	8.6 ± 0.1	16.1 ± 0.6	3.7 ± 0.8	13.1 ± 1.2	7.8 ± 0.5	13.8 ± 0.4
ΔE_{app}[a]	7.5 ± 0.6		9.4 ± 1.4		6.0 ± 0.6	
Dehydrogenation						
E_{app}	17.9 ± 0.2	24.8 ± 1.5	15.2 ± 1.4	23.3 ± 1.4	19.7 ± 0.8	34.5 ± 1.3
ΔE_{app}[a]	6.9 ± 1.5		8.1 ± 2.0		14.8 ± 1.5	

[a] Difference in the apparent activation energy in the presence and absence of CO, $\Delta E_{app} = E_{app}$(with CO) $- E_{app}$(without CO), in kcal mol^{-1}.

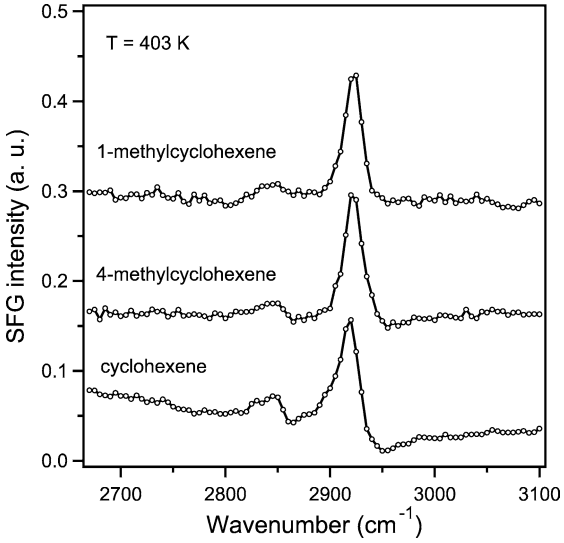

Fig. 3. SFG spectra taken at 403 K under 1.5 Torr 1-methylcyclohexene, 4-methylcyclohexene, or cyclohexene and 15 Torr H_2. Solid lines were drawn for visual aides.

contribute to the SFG bands. In particular, the transition dipole vector of the antisymmetric stretch of the CH_2 group at C_4 position is nearly perpendicular to the metal surface, giving rise to the strong SFG signal at 2920 cm^{-1}. In contrast, the transition dipole vector of the symmetric stretch is nearly parallel to the metal surface, giving rise to no SFG signal for the symmetric stretch as a consequence metal surface selection rules. Consequently, the SFG band at 2840 cm^{-1} is attributed to symmetric C–H stretches at C_3 and C_5 positions.

As shown in Fig. 3, SFG spectra of 1- and 4-methylcyclohexene adsorption are almost identical to those of cyclohexene, suggesting that these cycloalkenes have similar adsorption structures. Scheme 1b represents a proposed molecular structure of a methylcyclohexenyl (C_7H_{10}) as the surface intermediate responsible for the SFG spectra on adsorption of 1-methylcyclohexene. The rationale behind this proposal is the lack of vibrational stretching bands from a CH_3 group (2875 and 2950 cm^{-1} for symmetric and antisymmetric stretches, respectively) and a vinylic C–H (C=C–H, 3015 cm^{-1}) in the SFG spectra. The absence of the CH_3 stretching bands indicates that the CH_3 groups in 1- and 4-methylcyclohexene no longer exist upon adsorption. It is most likely that the CH_3 group was dehydrogenated to a CH_2 group, which was σ-bonded to the metal

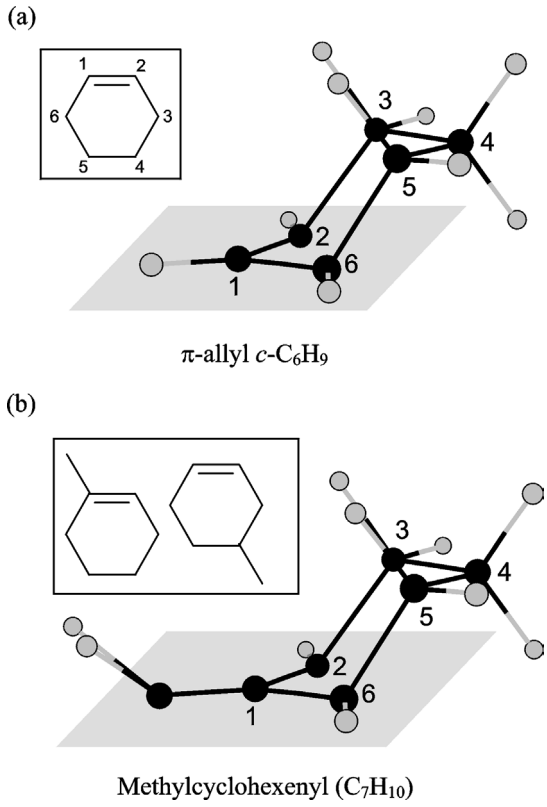

Scheme 1. Proposed surface intermediates: (a) π-allyl c-C_6H_9 and (b) methylcyclohexenyl.

surface. The absence of the vinylic C–H stretch indicates that 1- and 4-methylcyclohexene were σ-bonded by breaking the π bond. It is interesting to find that 1- and 4-methylcyclohexene produced the same surface intermediate despite their different positions of CH_3 group. The adsorption process for forming the methylcyclohexenyl intermediate is straightforward for 1-methylcyclohexene, which is initiated by physisorption via π bonding to the surface, followed by di-σ bonding and dehydrogenation of the CH_3 group. For 4-methylcyclohexene, double-bond migration of π bonded 4-methylcyclohexene is facile at room temperature in excess H_2 and may occur before the formation of σ-bonded methylcyclohexene, which eventually dehydrogenates to the methylcyclohexenyl intermediate [29]. Detailed analysis and discussion of the SFG spectra have been provided previously [30].

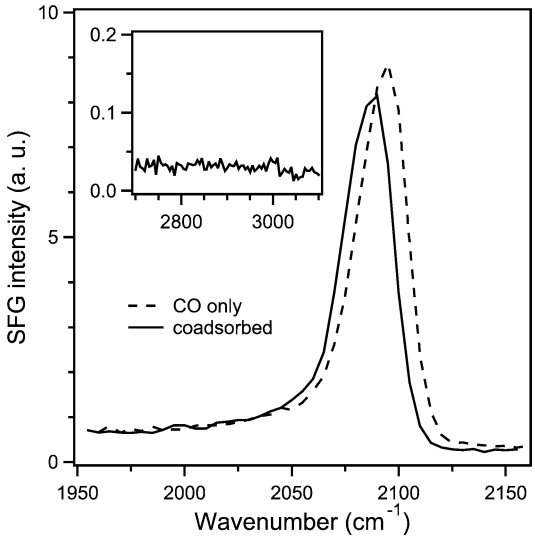

Fig. 4. SFG spectra taken at 300 K of 0.015 Torr CO (- - -), and 0.015 Torr CO with 1.5 Torr cyclohexene and 15 Torr H_2 (—). Inset is SFG signal between 2700 and 3100 cm^{-1} for the latter condition.

Fig. 4 shows the SFG vibrational spectra of surface species on Pt(111) at 300 K under 1.5 Torr cyclohexene, 15 Torr H_2, and 0.015 Torr CO. For comparison, the figure also shows the SFG spectrum of CO at 0.015 Torr in the absence of cyclohexene and H_2. The peak at 2090 cm^{-1} in the presence of CO, cyclohexene, and H_2 is associated with adsorbed atop CO [31–33]. No peak appears in the C–H stretching region, 2700–3000 cm^{-1} (inset). These results indicate that CO adsorption is more favorable than cycloalkene adsorption and that CO is the most abundant surface intermediate (masi).

4. Discussion

4.1. Substituent group influence on cycloalkene hydrogenation/dehydrogenation rates in the absence of CO

TORs and apparent activation energies (E_{app}) were determined for the hydrogenation/dehydrogenation of the three cycloalkenes (cyclohexene and 1-and 4-methylcyclohexenes) on Pt(111) in the absence of CO. In the absence of CO, TORs for both hydrogenation and dehydrogenation increased in the order of 1-methylcyclohexene < 4-methylcyclohexene < cyclohexene.

Several researchers have studied the effect of alkyl groups on alkene hydrogenation on metal surfaces [15,34]. In general, alkene hydrogenation rates on metal surfaces decrease with an increasing number of alkyl groups on the double bond. This effect can be explained by steric hindrance by the alkyl groups. It has been speculated that this steric effect disrupts alkene adsorption rather than the proceeding surface reactions [15]. The steric effect of an alkyl group on adsorption can explain the trend observed in this study. 1-Methylcyclohexene, in which a methyl group is attached to the C=C bond, should have the most difficulty adsorbing on the metal surface. Moreover, our finding that the dehydrogenation rate obeys the same tendency as the hydrogenation rate supports the notion that steric hindrance plays a significant role in the adsorption process. Kinetic studies of methylcyclohexene hydrogenation on Pd- and Pt-based catalysts have shown that the hydrogenation rate increases in the order of 1-methylcyclohexene < 3-methylcyclohexene < 4-methylcyclohexene, indicating that increasing proximity of the methyl group to the double bond increases the steric effect [3].

SFG results show that during catalytic reactions, the three cycloalkenes form surface intermediates with similar molecular structures. A similar or identical surface intermediate is created on adsorption of 1-methylcyclohexene and 4-methylcyclohexene. The proposed intermediate is methylcyclohexenyl (C_7H_{10}), as shown in Scheme 1b. This finding suggests that to form methylcyclohexenyl, molecularly adsorbed 4-methylcyclohexene is isomerized to 1-methylcyclohexene or 3-methylcyclohexene via double-bond migration. Double-bond migration of alkenes has been widely observed on various catalytic metal surfaces, including Pt, Pd, and Rh, and have been interpreted by two possible mechanisms [35]. The Horiuti–Polanyi mechanism involves the formation of the half-hydrogenated species, or (cyclo)alkyl species, whereas the mechanism proposed by Rooney and Webb involves the formation of a π-allyl species [36].

4.2. Temperature dependence of cyclohexene hydrogenation and dehydrogenation

The non-Arrhenius temperature behavior for both hydrogenation and dehydrogenation of cyclohexene in the presence and absence of CO led us to develop a mechanism that enabled the investigation of the effect of temperature on the proposed elementary reaction steps (see Appendix A). Hydrogenation and dehydrogenation were assumed to proceed through a mechanism in which hydrogen is sequentially removed or added stepwise to adsorbed cyclohexene. Using a quasi-empirical valence band (QVB) approach, Koel et al. [37] estimated the relative stability of adsorbed C_6 species on a Pt(111) surface for the dehydrogenation of cyclohexane to benzene. Koel et al. also included gas-phase cyclohexene in their model, enabling formulation of a reaction mechanism for both hydrogenation and dehydrogenation. The model provides information on the temperature dependence of the kinetic and thermodynamic parameters of the relevant elementary reaction steps. We demonstrate that the decreased rate at higher temperatures is related to decreased surface coverage of the reactive cycloalkene.

Fig. 1 shows that at ∼390 and ∼450 K, the turnover frequency for cycloalkene hydrogenation and dehydrogenation, respectively, reaches a maximum that is not related to thermodynamic equilibrium, poisoning, or transport effects. Over the entire temperature range studied, the conversion was kept low (<1%), while equilibrium conversions exceeded >60%. Poisoning effects were eliminated as a potential cause for the observed maxima, because rates were reproducible in a high-temperature experiment followed by a low-temperature experiment and vice versa. Potential mass transfer effects were eliminated by high recirculation rates (4 L min^{-1}) and the nonporous nature of the single crystal. The negative apparent activation en-

ergy is due to a change in surface coverage, where it eventually becomes low enough to retard the growth of the apparent rate constant even as the temperature is increased.

The apparent rate constant for hydrogenation ($k_{h,app}$) is written in Arrhenius form containing the equilibrium constant for cyclohexene adsorption (K_1), H_2 adsorption (K_{H_2}), the equilibrium constant for the surface reaction between adsorbed cyclohexene and adsorbed hydrogen (K_{2h}), and the kinetic rate constant for the proposed rate determining step (RDS), k_{3h} (see Appendix A). Therefore, the apparent activation energy for cycloalkene hydrogenation is a product of kinetic and thermodynamic quantities of several elementary steps: $E_{a,app} = E_{a,3h} + \Delta H_1 + \Delta H_{2h} + \Delta H_{H_2}$ because $k_{h,app} = A_{app} e^{-E_{a,app}/(RT)}$. At low temperatures, a positive apparent activation energy is measured for the hydrogenation reaction, and cycloalkene-derived species are identified on the surface. At these temperatures, the adsorption of cycloalkene and hydrogen is favorable, and the apparent rate constant increases with increasing temperature (i.e., normal Arrhenius behavior). Under high-pressure cycloalkene conditions and at low temperature, the zero-order dependence of the rate on cyclohexene suggests that the surface is covered with cycloalkene [5,38].

Fig. 1 shows that at ∼390 K, the hydrogenation rate reaches a maximum, and eventually the apparent activation energy for the hydrogenation of all cycloalkenes becomes negative at higher temperatures. The temperature of maximum activity coincides with the temperature at which C–H stretching bands corresponding to π-allyl c-C_6H_9 disappear in temperature-dependent SFG measurements performed under reaction conditions [12]. The decreased hydrogenation rate with increasing temperature is due to a decrease in H_2 adsorption and/or a decrease in cyclohexene adsorption. As the temperature increases to the point where $\theta_{C_6H_{10}}$ approaches zero, the most abundant surface species (*masi*) becomes a free site (see Appendix A). The change in *masi* causes a change in sign of the apparent activation energy, because the overall rate constant becomes $k_{h,app}$. To obtain a negative apparent activation energy, the true activation energy of the RDS must be smaller than the sum of the enthalpy of adsorption for the preceding quasi-equilibrated elementary steps. The low activation energy of the kinetically relevant step is evident from the observation that Pt(111) readily hydrogenates cyclohexene in excess hydrogen at room temperature. Although it is believed that the rate decreases because of a decrease in cycloalkene coverage (SFG observations), a comment on the influence of hydrogen is in order. In fact, bent or inverse Arrhenius plots have been measured for hydrocarbon reforming reactions [39], and it has been shown that this non-Arrhenius behavior is related to a hydrogen coverage effect [40]. As the reaction temperature increases at a constant hydrogen pressure, the hydrogen coverage decreases, as does the rate. Paál et al. [41] have shown that a maximum in rate is measured as function of hydrogen pressure at a constant temperature; the position of this maximum is related to the hydrogen content of the surface intermediate. This behavior suggests the need for an optimum hydrogen coverage that corresponds to zero-order hydrogen dependence. On either side of this maximum, H_2 and the reactive intermediate compete for empty surface sites. This site competition model has been used to explain observed rate maxima with H_2 pressure for alkane hydrogenolysis reactions on supported metal catalysts [42,43]. The dependence of the reaction rate on hydrogen has not been measured in this work, but it has been shown that if the maximum rate is found as a function of hydrogen pressure at different temperatures and the activation energy is calculated from the rates measured at the maxima, then "normal" Arrhenius plots are obtained [44].

Using the thermochemical parameters and reaction barriers for the hydrogenation reaction, it is easy to show, using the parameters of Koel et al. [37], that the apparent activation energy is negative under conditions of an essentially bare surface. In this case, the two scenarios (UHV conditions of Koel's calculations and high-temperature, high-pressure, low-coverage conditions) are very similar in terms of the surface density of adsorbates. The adsorption of cyclohexene (in a di-σ-bonded configuration) is nonactivated and exothermic ($\Delta H_1 = -17$ kcal mol^{-1}) [45] as are most chemisorption processes and becomes increasingly unfavorable as the temperature increases. The heat of adsorption of H_2 on a clean Pt(111) surface is estimated as 10–30 kcal mol^{-1} [46]. The second step is the surface reaction between the same adsorbed cyclohexene and hydrogen to form an adsorbed cyclohexyl species [Eq. (A.3)], which was determined to be exothermic ($\Delta H_{2h} = -12$ kcal mol^{-1}) [37]. Koel et al. [37] calculated the activation energy ($E_{a,3h}$) for the RDS as 17 kcal mol^{-1}. Combining these numbers and using a ΔH_{H_2} of -15 kcal mol^{-1}, the calculated apparent activation energy is negative (-27 kcal mol^{-1}) at high temperatures. Non-Arrhenius temperature behavior has also been documented for the vapor-phase hydrogenation of benzene over Fe/Al_2O_3. Yoon and Vannice [47] noted a maximum turnover frequency at ∼473 K for benzene pressures (20–100 Torr), which decreased to ∼453 K at lower benzene pressures (<3 Torr). The increased benzene partial pressure affords larger benzene coverage at higher temperatures.

A similar approach to gaining insight into the temperature dependence of the apparent activation for cycloalkene dehydrogenation uses the model of Koel et al. [37]. Fig. 1 demonstrates that the maximum rate for dehydrogenation shifts to higher temperatures (∼450 K) than that for hydrogenation. The increased temperature for maximum dehydrogenation activity is related to the overall endothermicity of the dehydrogenation reaction. Comparing the activity and selectivity on different Pt single crystals, Somorjai et al. [48] suggested that the hydrogenation/dehydrogenation reactions occur on distinct sites. Sermon [49] suggested that segregation of adsorbed H to high coordination sites makes the low-coordinated Pt sites capable of cyclohexene dehydrogenation. If low-coordination sites are responsible for dehydrogenation, then it is quite possible that these sites can stabilize cyclohexene adsorption at higher temperatures, and therefore the coverage of cyclohexene at these sites is greater than zero at temperatures where the hydrogenation rate has already begun to decrease. At some point, the rate of benzene formation begins to decrease with increasing temperature due to changes in cyclohexene surface cov-

erage. Fig. 1 shows that the apparent activation energy never becomes negative for the three cycloalkenes but that it does decrease with increasing temperature, suggesting that the cyclohexene coverage on sites responsible for dehydrogenation is in an intermediate range ($0 < \theta_{C_6H_{10}} < 1$), which decreases rapidly within the temperature range in which the slope of the Arrhenius plot starts to change. Eventually, the apparent activation energy will become negative at higher temperatures than those used in this experiment. An alternative explanation for the decreased dehydrogenation rate as a function of temperature is again related to hydrogen coverage and the "hydrogenative desorption" of products [44,50]. Temperature-programmed reaction/desorption (TPR/D) studies of cyclohexene dehydrogenation in UHV conditions on Pt single crystals have shown that hydrogen and benzene desorb at similar temperatures, suggesting that surface hydrogen is needed for benzene formation and subsequent desorption [51,52]. A similar phenomenon has been observed for the dehydrocyclization of n-C_6 hydrocarbons on Pt-black and a Pt/Al_2O_3 catalyst [50].

4.3. CO poisoning of cycloalkene hydrogenation and dehydrogenation

Adding CO to the reactant mixture led to a decreased rate (Fig. 1d–f) at the same temperature and increased apparent activation energy over a similar temperature range. The presence of CO in the gas phase caused increases in apparent activation energy of 8–10 kcal mol^{-1} for hydrogenation and 8–15 kcal mol^{-1} for dehydrogenation. If the hydrogenation and dehydrogenation occurred on distinct sites, as has been suggested [48,49], then it appears that CO bonds indiscriminately to both types of sites, based on similar increases in apparent activation energy for both reactions. Upon adsorption of 15 mTorr CO on Pt(111) at 300 K (Fig. 4), a vibrational feature for atop CO was observed at 2095 cm^{-1}, whereas coadsorption (1.5 Torr C_6H_{10}, 15 Torr H_2, 0.015 Torr CO) at 300 K led to no observable C–H resonance (inset in Fig. 4) and a slight red shift of the atop CO band (∼2090 cm^{-1}). The red shift may be due to the presence of either cyclohexene or carbon on the surface. This suggests that the dominant surface species is no longer a C_6 species, but rather CO. Inspection of Fig. 4 demonstrates that the area of the CO absorption band was relatively unchanged with the adsorption of cyclohexene. The coverage of CO on Pt(111) at these conditions was 0.68 ML, as determined by high-pressure STM studies [53,54]. Recent STM work showed that the coverage of CO does not change with the addition of ethylene to the surface, suggesting that CO molecules occupy atop and near-atop sites in the coadsorbed layer and ethylidyne replaces CO in three-fold hollow sites [53]. It is well known that CO favors atop binding on Pt(111); therefore, the fraction of CO in three-fold hollow sites is small, and the presence of ethylidyne requires relatively few CO molecules to desorb or diffuse to new adsorption sites. Similarly, it is believed that the adsorption of cyclohexene on a CO covered surface does not require CO desorption and that adsorbed C_6H_{10} is accommodated in the CO adlayer, potentially at a three-fold hollow site. This coadsorption behavior qualitatively explains why the coverage of carbon monoxide is unchanged in the presence of coadsorbed cyclohexene. At higher temperatures, the CO surface coverage will begin to decrease due to desorption. Assuming that the availability of free adsorption sites increases as CO begins to desorb and even though the adsorption of cyclohexene becomes thermodynamically unfavorable at higher temperatures, the increased number of free sites due to CO desorption allows the rate to increase in an Arrhenius fashion to much higher temperatures than were observed for the hydrogenation/dehydrogenation of cyclohexene in the absence of CO. This is demonstrated by the shift to higher peak temperatures for cyclohexene hydrogenation and dehydrogenation activity by ca. 50 and 55 K, respectively. Eventually, even in the case of the CO-poisoned experiments, the increased availability of sites cannot compensate for the unfavorable cycloalkene adsorption thermodynamics, and the rate decreases at higher temperatures.

The dependence of the reaction on CO partial pressure has not been measured on Pt(111), but CO inversely inhibits hydrogenolysis of methylcyclopropane [20] and the hydrogenation of ethylene on supported Pt/SiO_2 catalysts. The poisoning of cyclohexene hydrogenation/dehydrogenation with CO leads to an increased apparent activation energy due to a change in the most abundant surface species under reaction conditions (see Appendix A). In this case, CO will lead to an increase in the apparent activation energy due to the inclusion of the equilibrium constant for CO adsorption in the apparent rate constant, $k_{h,CO}$. The apparent activation energy now includes the adsorption of CO, causing an increase in the apparent activation energy; $E_{a,app}(CO) = E_{a,3h} + \Delta H_1 + \Delta H_{2h} + \Delta H_{H_2} - 2\Delta H_{CO}$, because $(-\Delta H_{CO})$ is a positive quantity. The saturation coverage of CO in the Torr pressure range is 0.68 ML [54], and the heat of adsorption is 10 kcal mol^{-1} by laser-induced thermal desorption (LITD) [55]. Analysis of the data in Table 1 confirms the difference in apparent activation energies in the presence and absence of CO (ΔE_{app}) is ∼9 kcal mol^{-1} (average of the hydrogenation and dehydrogenation ΔE_{app} for the three cycloalkenes), a value close to the CO heat of adsorption at saturation coverage. A similar increase of 10 kcal mol^{-1} in the apparent activation energy has been noted for the hydrogenation of ethylene in the absence and presence of CO in a similar pressure range on Pt(111) [21,22], Pt nanoparticle arrays [22,23], and supported Pt nanoparticle catalysts. The rate expression (see Appendix A) suggests that the apparent activation energy should increase by 20 kcal mol^{-1} if the measured ΔH_{ads} of CO at saturation coverage does not change in the presence of adsorbed C_6 species. The discrepancy between the experimentally measured activation energy in the presence of CO and that estimated by the rate expression may be a consequence of competitive adsorption between CO and C_6H_{10} on a single type of active site and of noncompetitive adsorption of H_2 on distinct surface sites. This two-site model can predict the observed inverse first-order CO kinetics and has been used to explain the kinetics of olefin hydrogenation reactions [56].

Alternatively, the change in the apparent activation energy may be due to a change in the RDS. Coadsorption studies of

ethylene–CO [53] and benzene–CO [57,58] on Pt(111) have shown that the overlayer structures are dense and that adsorbate mobility is severely hindered, suggesting that alkene adsorption may become difficult and even activated in some cases. In the case of the substituted cyclohexene molecules, initial adsorption on a crowded surface may become the rate-limiting step due to the steric hindrance of the CH_3 group. CO is probably located on bridge sites during C_6H_6–CO coadsorption [59], leading to a further decrease in the number of free sites relative to CO bonding at the atop position. Analysis of Table 1 demonstrates that ΔE_{app} for both hydrogenation and dehydrogenation (except for 4-methylcyclohexene hydrogenation) increases with substituted cyclohexenes. This suggests that the crowded surface exacerbates the influence of the bulky CH_3 group of the substituted cyclohexene. In the case of 4-methylcyclohexene, the double-bond migration may require a large ensemble of metal atoms not available on a CO-saturated surface.

5. Conclusion

In this study, the influence of substituent groups on the cycloalkene ring and their proximity to the C=C double bond were examined, and the influence of CO on the adsorption and kinetics of cycloalkene hydrogenation/dehydrogenation on Pt(111) was studied. For the three cycloalkenes studied, the TORs for both hydrogenation and dehydrogenation decreased, whereas activation energies for both reactions increased with the addition of substituent groups to the cycloalkene ring. These differences are attributed to steric effects. SFG surface vibrational spectroscopy measurements demonstrated that on adsorption, the three cycloalkenes formed a surface species with a similar molecular structure. Reaction rates for cycloalkene hydrogenation/dehydrogenation decreased significantly in the presence of adsorbed CO. Apparent activation energies increased by $\sim$9 kcal mol^{-1} in the presence of carbon monoxide. The difference in activation energy in the presence and absence of CO increases with substitution and the location of the substituent on the cycloalkene ring relative to the C=C double bond. SFG results demonstrated that CO excluded the cycloalkene from the surface. The poisoning of cycloalkene hydrogenation/dehydrogenation with CO led to an increased apparent activation energy due to a change in the most abundant surface species under reaction conditions. This study may lend insight into the design of CO-tolerant hydrocarbon conversion catalysts.

Acknowledgments

This work was supported by the Office of Energy Research, Office of Basic Energy Sciences, Chemical Sciences Division, U.S. Department of Energy under contract DE-AC02-05CH11231. R.M.R. acknowledges financial support from the Ford Motor Corporation through the Ford Catalysis Fellowship administered by the Berkeley Catalysis Center.

Appendix A. Proposed cycloalkene hydrogenation mechanism and derivation of rate expression

This appendix proposes a reaction mechanism for cyclohexene hydrogenation and derives a rate equation to explain non-Arrhenius behavior at high temperature and the increase in apparent activation energy in the presence of CO.

A.1. Langmuir–Hinshelwood mechanism for cyclohexene hydrogenation

The proposed mechanism for cycloalkene hydrogenation comprises the following elementary reaction steps in which C_6 intermediates are sequentially hydrogenated. Adsorption of cyclohexene is assumed to be quasi-equilibrated, requiring a free site (*) for adsorption. The identity of this site is not known; it may consist of a single atom or an ensemble of atoms:

$$H_2 + 2* \overset{K_{H_2}}{\rightleftharpoons} 2H*, \tag{A.1}$$

$$C_6H_{10} + * \overset{K_1}{\rightleftharpoons} C_6\,H_{10}*, \tag{A.2}$$

$$C_6H_{10}* + H* \overset{K_{2h}}{\rightleftharpoons} C_6H_{11}* + *, \tag{A.3}$$

$$C_6H_{11}* + H* \xrightarrow{k_{3h}} C_6H_{12}* + *. \tag{A.4}$$

Adsorbed cyclohexene is hydrogenated to yield adsorbed cyclohexyl (C_6H_{11}*) species. Both C_6H_{10} adsorption and its hydrogenation to C_6H_{11}* are reversible, based on the observation that d_1-C_6H_{10} is observed in the gas phase during C_6H_{10}/D_2 experiments due to the dehydrogenation of d_1-C_6H_{11} species, assuming that H–D exchange does not occur [60,61]. According to Koel et al. [37], C_6H_{11}* is the most stable adsorbed C_6 species in the conversion of cyclohexene to cyclohexane. This choice of RDS is in accord with the proposed RDS for benzene hydrogenation [47]. The rate of cyclohexene hydrogenation is written as

$$r_{C_6H_{12}} = k_{3h}[C_6H_{11}*][H*], \tag{A.5}$$

where the concentration of adsorbed hydrogen is determined from the equilibrium between adsorbed H and gas-phase H_2, $[H*] = K_{H_2}^{1/2}[H_2]^{1/2}[*]$, and $[C_6H_{11}*]$ is calculated from the quasi-equilibrium of the cycloalkene adsorption and reaction steps (A.2) and (A.3). Replacing the concentration of adsorbed cyclohexyl species in the rate expression with reactant partial pressures, the RDS becomes

$$r_{C_6H_{12}} = K_1K_{2h}K_{H_2}k_{3h}\,[C_6H_{10}][H_2][*]^2. \tag{A.6}$$

The number of free sites [*] is determined from an overall site balance. The total number of sites, [L], is $[L] = [*] + [C_6H_{10}*]$, leading to a Langmuir–Hinshelwood-type rate expression for the formation of cyclohexane,

$$r_{C_6H_{12}} = \frac{k_{h,app}[C_6H_{10}][H_2]}{\left(1 + K_1[C_6H_{10}]\right)^2}, \tag{A.7}$$

where $k_{h,app} = K_1 K_{2h} K_{H_2} k_{3h}[L]$. Cyclohexene is considered a major surface species due to the favorable adsorption thermodynamics at low temperatures ($300\ K \leqslant T \leqslant 400\ K$), the high cyclohexene gas-phase pressure, and the zero-order cyclohexene kinetics reported by a number of researchers [5,38]. The foregoing rate expression allows for the dependence on C_6H_{10} pressure to vary from -1 to first order. At low temperatures, the $K_1[C_6H_{10}]$ becomes considerably larger than unity and the rate expression becomes

$$r_{C_6H_{12}} = \frac{k_{h,app}[H_2]}{K_1^2[C_6H_{10}]},$$

where the overall rate constant is $k_{h,app}/K_1^2 (= K_{2h} K_{H_2} k_{3h}[L]/K_1)$, which increases with increasing temperature and leads to a positive apparent activation energy. As the temperature increases, the $K_1[C_6H_{10}]$ in the denominator of Eq. (A.7) decreases, leaving a free site as the *masi*, and the rate expression becomes $r_{C_6H_{12}} = k_{h,app}[C_6H_{10}][H_2]$ as cyclohexene adsorption is not favored. Under these conditions, $k_{h,app}$ decreases with increasing temperature if the product of equilibrium constants, $K_1 K_{2h} K_{H_2}$ decreases with temperature more quickly than k_{3h} increases. The lumped equilibrium constants are exothermic and thus decrease with increasing temperature.

A.2. Influence of CO on proposed rate equation

The addition of mTorr pressure of CO in the gas phase leads to adsorption/desorption equilibrium between gas-phase CO and adsorbed CO (i.e., $CO + * \leftrightharpoons CO*$). Favorable CO adsorption thermodynamics leads to a change in the *masi*, such that the site balance becomes $[L] = [CO*] = K_{CO}[CO][*]$ and the rate expression for cyclohexene hydrogenation in the presence of CO becomes

$$r_{C_6H_{12}} = \frac{k_{h,CO}[C_6H_{10}][H_2]}{[CO]^2}, \tag{A.8}$$

where $k_{h,CO} = k_{h,app}/K_{CO}^2$. This rate expression predicts an inverse second-order inhibition of CO on the overall hydrogenation kinetics (dehydrogenation as well). Therefore, it is possible that the RDS changes in the presence of CO and the adsorption of the cycloalkene becomes rate determining [Eq. (A.2)], leading to a rate expression with an inverse first-order dependence on carbon monoxide. In this case, $k_{h,app}$ would depend on the thermodynamics of cycloalkene and carbon monoxide adsorption. Alternatively, a two-site mechanism, in which H_2 adsorption is noncompetitive and C_6H_{10}–CO adsorption is competitive, would predict the observed inverse first-order dependence in carbon monoxide [56].

References

[1] M.A. Aramendia, V. Borau, I.M. Garcia, C. Jimenez, A. Marinas, J.M. Marinas, F.J. Urbano, J. Mol. Catal. 151 (2000) 261.
[2] Z. Xu, B.C. Gates, J. Catal. 154 (1995) 335.
[3] R.A.W. Johnstone, J. Liu, L. Lu, D. Whittacker, J. Mol. Catal. A 191 (2003) 289.
[4] S.D. Jackson, G.J. Kelly, S.R. Watson, R. Gulickx, Appl. Catal. A 187 (1999) 161.
[5] M. Boudart, C.M. McConica, J. Catal. 117 (1989) 33.
[6] Z. Paàl, in: G.J. Antos, A.M. Aitani (Eds.), Catalytic Naphtha Reforming, second ed., Marcel Dekker, New York, 2004, p. 35.
[7] J.A. Rodriguez, C.T. Campbell, J. Catal. 115 (1989) 500.
[8] F.C. Henn, A.L. Diaz, M.E. Bussell, M.B. Hugenschmidt, M.E. Domagala, C.T. Campbell, J. Phys. Chem. 96 (1992) 5965.
[9] C.L. Pettiette-Hall, D.P. Land, R.T. McIver, J.C. Hemminger, J. Am. Chem. Soc. 113 (1991) 2755.
[10] C.L.A. Lamont, M. Borbach, R. Martin, P. Gardner, T.S. Jones, H. Conrad, A.M. Bradshaw, Surf. Sci. 374 (1997) 215.
[11] W.L. Manner, G.S. Girolami, R.G. Nuzzo, J. Phys. Chem. B 102 (1998) 10295.
[12] M. Yang, K. Chou, G.A. Somorjai, J. Phys. Chem. B 107 (2003) 5267.
[13] S.M. Davis, G.A. Somorjai, J. Catal. 65 (1980) 78.
[14] S.M. Davis, G.A. Somorjai, Surf. Sci. 91 (1980) 73.
[15] M. Kraus, in: G. Ertl, H. Knozinger, J. Weitkamp (Eds.), Handbook of Heterogeneous Catalysis, VCH, Weinheim, 1997, p. 1051.
[16] S. Siegel, B. Dmuchovsky, J. Am. Chem. Soc. 84 (1961) 3132.
[17] S. Siegel, G. Smith, J. Am. Chem. Soc. 82 (1960) 6082.
[18] Z. Paál, G.A. Somorjai, in: G. Ertl, H. Knozinger, J. Weitkamp (Eds.), Handbook of Heterogeneous Catalysis, VCH, Weinheim, 1997, p. 1084.
[19] D.E. Damiani, J.B. Butt, J. Catal. 94 (1985) 218.
[20] D.E. Damiani, J.B. Butt, J. Catal. 94 (1985) 203.
[21] P. Chen, K.Y. Kung, Y.R. Shen, G.A. Somorjai, Surf. Sci. 494 (2001) 289.
[22] K.S. Hwang, M. Yang, J. Zhu, J. Grunes, G.A. Somorjai, J. Mol. Catal. A 204 (2003) 499.
[23] J. Grunes, J. Zhu, M.C. Yang, G.A. Somorjai, Catal. Lett. 86 (2003) 157.
[24] Y.R. Shen, The Principles of Nonlinear Optics, Wiley, New York, 1984, p. 67.
[25] Y.R. Shen, Nature 337 (1989) 519.
[26] Y.R. Shen, Annu. Rev. Phys. Chem. 40 (1989) 327.
[27] M. Yang, D.C. Tang, G.A. Somorjai, Rev. Sci. Instrum. 74 (2003) 4554.
[28] K.Y. Kung, P. Chen, F. Wei, G. Rupprechter, Y.R. Shen, G.A. Somorjai, Rev. Sci. Instrum. 72 (2001) 1806.
[29] P.B. Wells, G.R. Wilson, Discuss. Faraday Soc. 40 (1966) 237.
[30] M. Yang, G.A. Somorjai, J. Phys. Chem. B 108 (2004) 4405.
[31] G. Rupprechter, T. Dellwig, H. Unterhalt, H.-J. Freund, J. Phys. Chem. B 105 (2001) 3797.
[32] X. Su, P.S. Cremer, Y.R. Shen, G.A. Somorjai, Phys. Rev. Lett. 77 (1996) 3858.
[33] C. Klunker, M. Balden, S. Lehwald, W. Daum, Surf. Sci. 360 (1996) 104.
[34] M.L. Burke, R.J. Madix, J. Am. Chem. Soc. 113 (1991) 4151.
[35] G.A. Olah, A. Molnar, Hydrocarbon Chemistry, second ed., Wiley, Hoboken, 2003, p. 622.
[36] J.J. Rooney, G. Webb, J. Catal. 3 (1964) 488.
[37] B.E. Koel, D.A. Blank, E.A. Carter, J. Mol. Catal. A 131 (1998) 39.
[38] D.J.L. O'Rear, M. Boudart, J. Catal. 94 (1985) 225.
[39] S.M. Davis, F. Zaera, G.A. Somorjai, J. Catal. 85 (1984) 206.
[40] Z. Paál, J. Catal. 91 (1985) 181.
[41] Z. Paál, P.G. Menon, Catal. Rev.-Sci. Eng. 25 (1983) 223.
[42] G.C. Bond, J.C. Slaa, Catal. Lett. 23 (1994) 293.
[43] G.C. Bond, J.C. Slaa, J. Mol. Catal. A: Chem. 98 (1995) 81.
[44] A. Wootsch, Z. Paál, J. Catal. 205 (2002) 86.
[45] C. Xu, B.E. Koel, Surf. Sci. 304 (1994) 349.
[46] I. Toyoshima, G.A. Somorjai, Catal. Rev. Sci. Eng. 19 (1) (1979) 105.
[47] K.J. Yoon, M.A. Vannice, J. Catal. 82 (1983) 457.
[48] K.R. McCrea, G.A. Somorjai, J. Mol. Catal. A 163 (2000) 43.
[49] P.A. Sermon, G. Georgiades, M.M.A. Martin-Luengo, Proc. R. Soc. London, Ser. A 410 (1987) 353.
[50] H. Zimmer, V.V. Rozanov, A.V. Sklyarov, Z. Paál, Appl. Catal. 2 (1982) 51.
[51] A.V. Teplyakov, B.E. Bent, J. Phys. Chem. B 101 (1997) 9052.
[52] M.-C. Tsai, C.M. Friend, E.L. Muetterties, J. Am. Chem. Soc. 104 (1982) 2539.
[53] D.C. Tang, K.S. Hwang, M. Salmeron, G.A. Somorjai, J. Phys. Chem. B 108 (2004) 13300.
[54] E. Kruse Vestergaard, P. Thostrup, T. An, E. Lægsgaard, I. Stensgaard, B. Hammer, F. Besenbacher, Phys. Rev. Lett. 88 (2002) 259601.

[55] E.G. Seebauer, A.C.F. Kong, L.D. Schmidt, Surf. Sci. 176 (1986) 134.
[56] G.B. Rogers, M.M. Lih, O.A. Hougen, AIChE J. 12 (1966) 369.
[57] M.A. Van Hove, R.F. Lin, D.F. Ogletree, G.S. Blackman, C.M. Mate, G.A. Somorjai, J. Vac. Sci. Technol. A 5 (1987) 692.
[58] H.A. Yoon, M. Salmeron, G.A. Somorjai, Surf. Sci. 373 (1997) 300.
[59] M.A. Van Hove, G.A. Somorjai, J. Mol. Catal. A 131 (1998) 243.
[60] A.P.I. Fási, T. Katona, M. Bartók, J. Catal. 167 (1997) 215.
[61] A.V. Teplyakov, B.E. Bent, J. Chem. Soc., Faraday Trans. 91 (1995) 3645.